

The key-lock mechanism in nematic colloidal dispersions

N.M. Silvestre¹, P. Patrício^{1,2}, and M.M. Telo da Gama¹

¹Departamento de Física da Faculdade de Ciências and Centro de Física Teórica e Computacional
Universidade de Lisboa, Avenida Professor Gama Pinto 2, P-1649-003 Lisboa Codex, Portugal

²Instituto Superior de Engenharia de Lisboa
Rua Conselheiro Emídio Navarro 1, P-1949-014 Lisboa, Portugal

(October 2003)

We consider the interaction of two-dimensional colloids, in nematic liquid crystals, with walls or geometrical boundaries. The interactions between colloidal disks and flat walls, with homeotropic boundary conditions, are always repulsive. The repulsions may be turned into strong attractions at structured or sculpted walls with cavities, matching closely the shape and size of the colloids. This key-lock type of interaction is analyzed in detail for spherocylindrical cavities of various length to breath ratios, by minimizing the Landau-de Gennes free energy functional of the orientational order parameter. We find that the attractions occur only for walls with cavities within a small range of the colloidal size and for a narrow range of orientations around the wall's symmetry axis.

I. INTRODUCTION

In the last ten years, there has been continued interest in colloidal dispersions in nematics and other liquid crystalline phases (LCs) owing to their novel, complex behavior [1]. The behavior of spherical isotropic particles in a nematic matrix depends upon (i) the elastic constants of the nematic, (ii) the size of the particle, and (iii) the boundary conditions at the particle and at the container, including the anchoring energy of the nematicogenic molecules and possibly on additional (generic) surface tension effects. All of these contributions are temperature dependent and their combination leads to complex anisotropic long-ranged colloidal interactions [2–4]. These were reported to lead to a variety of novel self-organized colloidal structures, such as linear chains [5,6], periodic lattices [7], anisotropic clusters [8], and cellular structures [9] that are stabilized, in general, by topological defects.

More recently, two-dimensional (2D) inverted nematic emulsions were also studied and a similar behavior has been reported [10–14]. In particular, Landau-de Gennes (LdG) theory predicts that the stable configuration for a colloidal disk, with strong homeotropic anchoring, is always a pair of 1/2 charge topological defects [15] and thus that the long-range interaction between 2D colloids is quadrupolar for any sized particles [14].

The interactions between colloids and the nematic-isotropic (NI) interface were also investigated [16,17]. These include specific contributions from the liquid crystal matrix due to deformation of the director field close to the particles and/or the interface, and a generic contribution due to wetting and surface tension effects. At equilibrium, strong distortions of the planar interfacial region, on the scale of the colloidal radius, were found to occur with the colloid being partially wrapped by the interface. The effective colloid-interface interaction was found to be rather complex and simple scaling analyses for flat interfaces were shown to fail badly [17].

At the same time impressive technological advances allowed the controlled fabrication of micro-patterned and structured surfaces, on the nanometer to the micrometer scales [18]. The interplay between surface geometry and orientational order required to understand the phenomenology of LCs on patterned substrates, on these scales, is largely unexplored. In this article we embark on a systematic investigation of the effects of geometry and orientational order on the interaction between colloids and solid surfaces. In particular, we investigate the interaction between 2D colloids and hard surfaces, ranging from flat to structured on the colloidal scale.

We study the interaction between one disk and flat as well as structured walls, using the method of images and/or by minimizing the LdG free energy numerically. For a single cavity, sculpted on a flat surface, we find that the repulsion at flat walls may be turned into a rather strong attraction, as a result of the interplay between geometry and orientational order. This effect occurs at cavities with sizes in the colloidal range resembling the so-called *key-lock* mechanism.

In section II, we review briefly the Landau-de Gennes theory and in section III we present the results for the interaction between one disk and a flat wall. In section IV we consider the interaction of colloidal disks with cavities sculpted on flat walls. We investigate the effects of the size and shape of the cavity and of the colloidal orientation with respect to the cavity's symmetry axis. Finally, in section V we summarize our results and make some concluding remarks.

II. LANDAU-DE GENNES FUNCTIONAL

In what follows we consider a two-dimensional nematic liquid crystal. On average, the molecules are aligned along one common direction described by the director \mathbf{n} and the tensor order parameter is defined as

$Q_{\alpha\beta}(\mathbf{r}) = Q(\mathbf{r})(n_\alpha(\mathbf{r})n_\beta(\mathbf{r}) - \delta_{\alpha\beta}/2)$ [19]. In the situations to be investigated, the distances over which significant variations of $Q_{\alpha\beta}$ occur are much larger than molecular dimensions. Thus we neglect density variations. The free energy density is then written in terms of invariants of \mathbf{Q} and its derivatives and is known as the Landau-de Gennes free energy,

$$F[Q_{\alpha\beta}, \nabla Q_{\alpha\beta}] = \int_{\Omega} d^2r \left[-\frac{A}{2} \text{Tr}\{\mathbf{Q}^2\} + \frac{C}{4} \text{Tr}\{\mathbf{Q}^2\}^2 + \frac{L}{2} \nabla_\gamma Q_{\alpha\beta} \nabla^\gamma Q^{\alpha\beta} \right] \quad (1)$$

where we used the one elastic constant approximation. Tr denotes the trace operation, Ω is the area of the 2D system, A and C are bulk constants and L is the elastic constant. Stability requires $C > 0$. In the nematic phase ($A > 0$) and the equilibrium orientational order parameter is $Q_{\text{bulk}} = \sqrt{2A/C}$. We use finite elements with adaptive meshing, as described in [13], to minimize the Landau-de Gennes free energy functional.

III. THE FLAT WALL

We start by considering the interaction of a colloidal disk, of radius a , with a flat wall. In [20] the *method of images* was used to study the interaction of a disclination with a planar wall. We used the same method to study the long-range interaction of a colloidal disk with a flat wall. We assumed homeotropic boundary conditions at the wall and at the disk's surface, and took the far field \mathbf{n}_0 perpendicular to the wall. It is easy to check, that the long-range disk-wall interaction is identical to the interaction between the disk and its virtual image. Thus the long-range disk-wall interaction is always repulsive and decays as R^{-4} [14], where R is the distance of the center of the disk to the wall.

In Fig. 1 we plot the interaction energy as a function of R , for all R . As noted above, the long-range interaction is always repulsive and we find that the repulsion increases as the colloid approaches the wall. This increased short-range repulsion is associated with the strong distortion of the nematic matrix between the (flat) wall and the (curved) disk, due to the competition between the fixed anchoring conditions at the wall and at the disk's surface. As a result the pair of $1/2$ defects surrounding the disk are displaced with respect to their (symmetrical) equatorial position in isolated disks. The distortion of the nematic matrix extends from the wall up to the line joining the defects and under these circumstances the elastic free energy is minimized if the defects move closer to the wall (see Fig. 2).

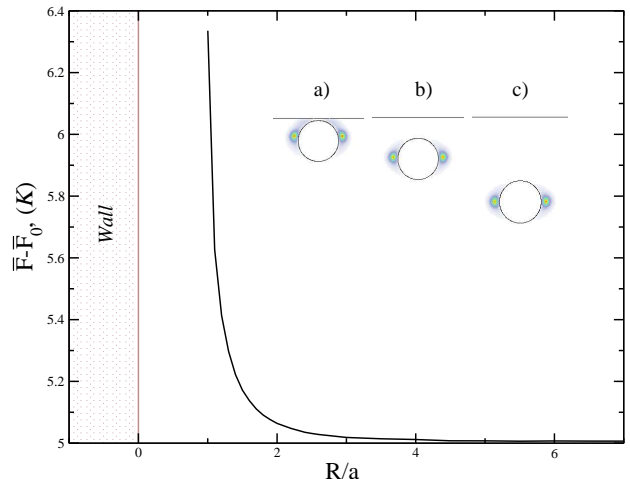


FIG. 1. Reduced interaction energy as a function of the distance R from the center of the colloid, of radius a , to the wall. $\bar{F} = F/K$, where $K = 2LQ_{\text{bulk}}$ is the Frank elastic constant, and F_0 is the Landau-de Gennes free energy of the system without colloid. The inset illustrates the order parameter maps at different R . a) $R/a = 1.1$; b) $R/a = 2.0$; c) $R/a = 4.0$. The nematic order parameter varies between $Q = Q_{\text{bulk}}$ (white regions) and $Q = 0$ (colored regions).

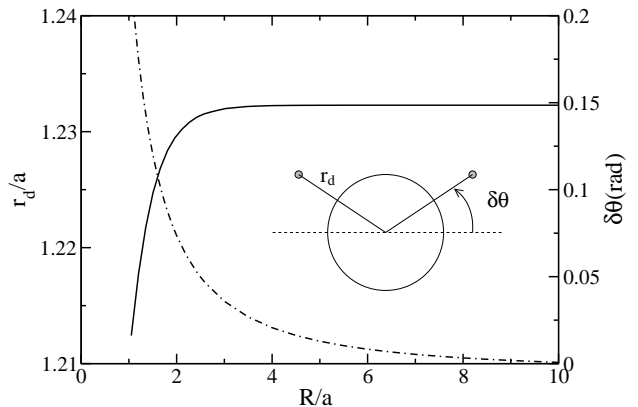


FIG. 2. Defect distance r_d from the center of the disk (continuous line) and defect orientation $\delta\theta$ (dash-dotted line), with respect to the orientation in isolated disks, as a function of R .

IV. STRUCTURED WALL

We now consider a sculpted cavity on an otherwise flat wall, as shown in Fig. 3. The cavity is spherocylindrical of radius r and half-length or depth, d . Homeotropic boundary conditions are set at the wall and at the colloidal surface. The far field \mathbf{n}_0 is again perpendicular to the wall. To avoid the presence of defects at the corners these were smoothed as shown in Fig. 6.

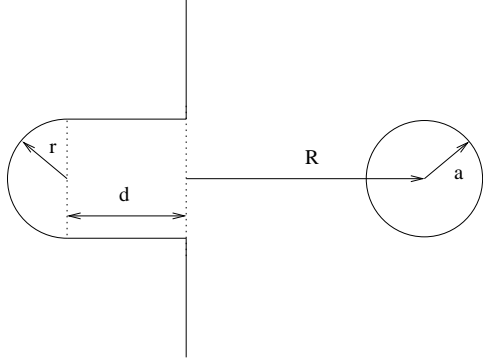


FIG. 3. Structured wall: geometry and notation

The image method cannot be applied in this case and thus analytical expressions for the long-range interaction between the disk and the cavity are not known. In addition the non-linearities, that come into play as the colloid approaches the cavity, are more complex. The free energy is minimized numerically as before, using finite elements with adaptive meshing [13].

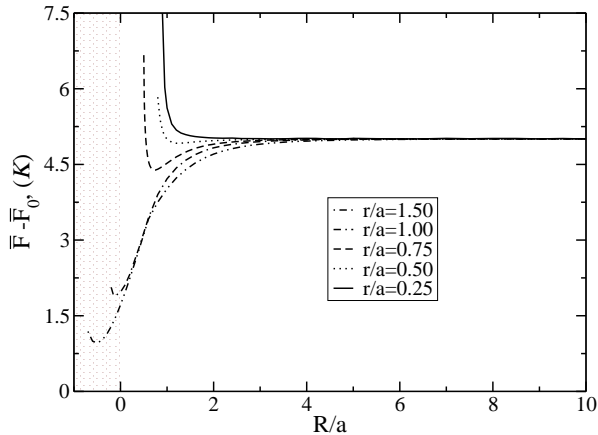


FIG. 4. Reduced interaction energy as a function of the distance, R , of the center of the colloid to the midpoint of the cavity's entrance, for several widths ($r/a = 0.25, 0.50, 0.75, 1.00, 1.50$). The depth is $d/a = 0.01$.

We start by considering a very shallow cavity, with $d/a = 0.01$ (see Fig. 4). If the cavity is also sufficiently narrow ($r/a < 0.25$) the colloid-wall interaction is very similar to the interaction with the flat wall. As the radius of the cavity increases an attraction with a well defined minimum eventually occurs. The minimum is inside the cavity if the width is larger than the colloidal radius, $r/a > 1$.

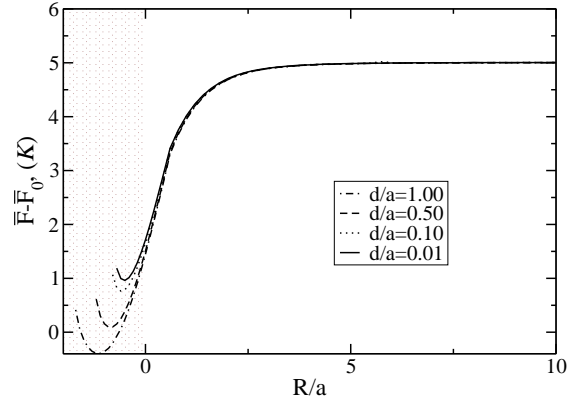


FIG. 5. Reduced interaction energy as a function of the distance R , for several depths ($d/a = 0.01, 0.10, 0.50, 1.00$). The radius of the cavity is $r/a = 1.5$.

We proceed by studying the effect of the cavity's depth d . The radius is set at $r/a = 1.5$ (corresponding to the lowest energy of all the cavities studied, as shown in Fig. 4). In Fig. 5 we plot the reduced interaction energy, as a function of the distance R , for cavities with depths ($d/a = 0.01, 0.10, 0.50, 1.00$). Clearly, increasing d lowers the interaction energy minimum by shifting it into the cavity. The distortion of the nematic matrix is minimal when the colloid is well within the cavity.

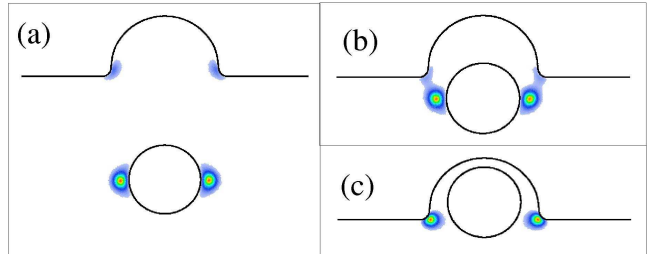


FIG. 6. Order parameter maps for a cavity with $r/a = 1.5$ and $d/a = 0.01$, and different colloidal separations R . (a) $R/a = 3.0$; (b) $R/a = 0.6$; (c) $R/a = -0.5$. The nematic order parameter varies between $Q = Q_{\text{bulk}}$ (white regions) and $Q = 0$ (colored regions).

In Fig. 6 we plot the nematic order parameter maps for a cavity with $r/a = 1.5$ and $d/a = 0.01$, and different colloidal separations, R . As the colloid approaches the cavity, the two $1/2$ defects move towards the corners and merge with the distorted region of the nematic matrix in the absence of the colloid (see Fig. 6). As d increases, the colloid moves deeper into the cavity; the defects are further localized near the corners leading to a significant reduction in the elastic free energy, as shown in Fig. 5. Fig. 6(c) corresponds to the minimal free energy, at a separation $R/a = -0.5$, where the force on the colloid vanishes.

However, if we increase the cavity depth further, the nematic director configuration suddenly changes, leading again to a strong colloidal repulsion. In fact, due to the homeotropic boundary conditions, there is a critical depth, d_c , beyond which the stable nematic configuration of the empty cavity exhibits two topological defects. One topological defect is inside the cavity, near the cap, while the other is pinned near one of the corners (see Fig. 7). This broken symmetry configuration is two-fold degenerate. Along the cavity 'neck' the nematic director is now almost constant and it will be disrupted by a colloidal disk. This is reflected by the existence of a free energy barrier that prevents the penetration of the particle. This barrier will vanish for cavities that are sufficiently wide to allow smooth deformations of the director field when the colloid is inserted.

The critical depth d_c may be estimated by simple dimensional arguments. For smooth deformations, the elastic free energy of the nematic in the cavity is proportional to Kd/r . By contrast, when defects are present the free energy scales as $\pi q^2 K$, where q is the defect topological charge. Thus the critical depth is $d_c \propto \pi q^2 r$.

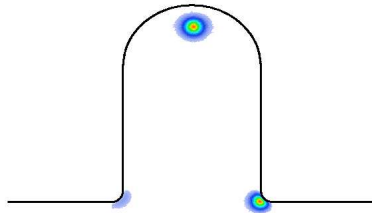


FIG. 7. Order parameter map for a nematic filled cavity of depth $d \gg d_c$. The nematic order parameter varies between $Q = Q_{\text{bulk}}$ (white regions) and $Q = 0$ (colored regions).

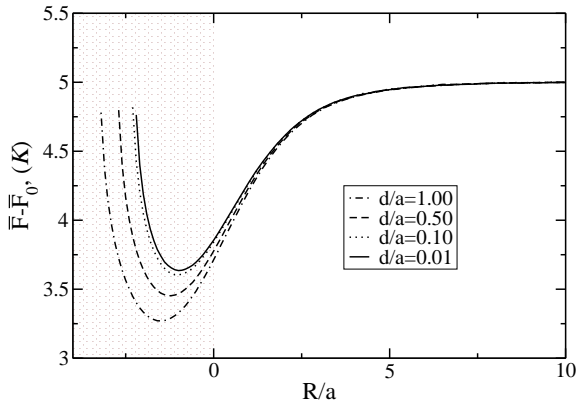


FIG. 8. Reduced interaction energy as a function of the separation R for several depths ($d/a = 0.01, 0.10, 0.50, 1.00$). The radius of the cavity is $r/a = 3.0$.

In Fig. 8 we plot the reduced interaction energy, as a

function of R , for a cavity with radius $r/a = 3.0$ and several depths ($d/a = 0.01, 0.10, 0.50, 1.00$). As in the previous case, increasing d lowers the minimum of the interaction energy and shifts its position inwards. However, the relative variation is not as strong as for $r/a = 1.5$. The attraction is much weaker for the wider cavity. Clearly, when the radius of the cavity is very large, the long-range interaction between the disk and a structured wall is similar to the interaction of the disk with a flat wall.

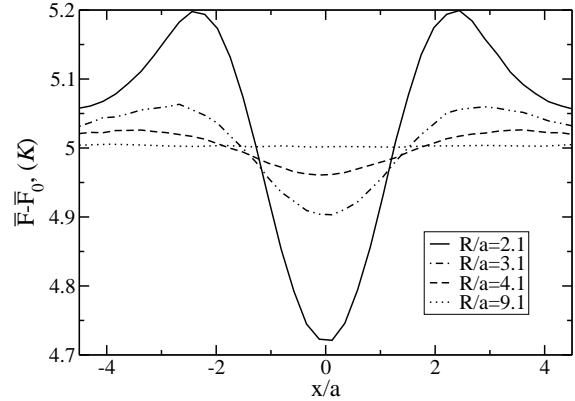


FIG. 9. Reduced interaction energy along four lines parallel to the wall ($R/a = 2.1, 3.1, 4.1, 9.1$) as a function of the lateral distance from the cavity, x/a . The radius and depth of the cavity are $r/a = 1.5$ and $d/a = 1.00$, respectively.

The results so far considered the interaction between colloidal disks and skulpted walls along the symmetry axis of the cavity (see Fig. 3). In the following we consider the interaction energy along different directions. In Fig. 9 we plot the interaction energy along four lines parallel to the wall ($R/a = 2.1, 3.1, 4.1, 9.1$), as a function of the lateral distance from the cavity, x/a , for a cavity with $r/a = 1.5$ and $d/a = 1.00$. Note that the attraction is limited to a certain angle that depends on the colloidal separation, R . Outside that region, the colloid is repelled by the wall. The repulsion has contributions from the flat wall repulsion and from the repulsion from the cavity corners. Indeed, a strong variation of the interaction energy as the disk approaches the cavity's corners is seen in Fig. 9.

We conclude that the colloid will be trapped by an appropriately sized cavity if and only if it is (driven) inside its 'cone' of attraction.

V. CONCLUSIONS

We studied the interaction of a colloidal disk in a 2D nematic, with a flat wall with homeotropic boundary conditions and found that it is purely repulsive and decays at long-range as R^{-4} . By structuring the surface with a

cavity that is similar in size and shape to the colloid we found a robust key-lock mechanism, capable of turning the repulsion into an attraction that is large enough to be effective in trapping or capturing colloidal particles.

This key-lock mechanism is clearly dependent on the geometry of both the colloid and the cavity and its effectiveness for other colloidal shapes will be addressed in future work. Another relevant question that is left open is the existence of a similar effect at soft (deformable) walls. This will allow contact with recent results at NI interfaces where colloids were found to be trapped through a mechanism that is somewhat more complex, since the bending of the interface results from the colloidal interactions [17].

Lastly, we note that the key-lock mechanism has features reminiscent of the process of wrapping colloids by a membrane [21,22]. It is likely that the major factors determining this wrapping process are most simply illustrated for the type of hard structured walls considered in this work. However, a detailed comparison of hard and soft surfaces requires further analysis based on the LdG approach and/or effective Hamiltonian models, in order to assess (among other things) the role of thermal fluctuations.

We end with the remark that our results for the 2D key-lock mechanism are applicable to a particular 3D system, consisting of long rod-like colloids with their major axes parallel to a planar surface. Three dimensional effects, such as the biaxiality at the defect cores, are small [23] and thus the key-lock mechanism reported here should be valid for 3D systems where the non-uniformity is (quasi) two-dimensional.

[1] H. Stark, Phys. Rep. **351**, 387 (2001).
 [2] S. Ramaswamy, R. Ninyananda, V.A. Raghunathan, and J. Prost Mol. Cryst. Liq. Cryst. **288**, 175 (1996).
 [3] P. Poulin, V. Cabuil, and D. A. Weitz, Phys. Rev. Lett. **79**, 4862 (1997).
 [4] T. C. Lubensky, D. Pettey, N. Currier, and H. Stark, Phys. Rev. E **57**, 610 (1997).
 [5] P. Poulin, H. Stark, T. C. Lubensky, and D. A. Weitz, Science **275**, 1770 (1997).
 [6] J.-C. Loudet, P. Barois, and P. Poulin, Nature **407**, 611 (2000).
 [7] V. G. Nazarenko, A. B. Nych, and B. I. Lev, Phys. Rev. Lett. **87**, 075504 (2001).
 [8] P. Poulin, N. Frances, and O. Mondain-Monval, Phys. Rev. E **59**, 4384 (1999).
 [9] S. P. Meeker, W. C. K. Poon, J. Crain, and E. M. Terentjev, Phys. Rev. E **61**, R6083 (2000).
 [10] D. Pettey, T. C. Lubensky, and D. R. Link, Liq. Cryst. **25**, 5 (1998).
 [11] P. Cluzeau, P. Poulin, G. Joly, and H. T. Nguyen, Phys. Rev. E **63**, 031702 (2001).
 [12] P. Cluzeau, V. Bonnand, G. Joly, V. Dolganov, and H. T. Nguyen, Eur. Phys. J. E **10**, 231 (2003).
 [13] P. Patrício, M. Tasinkevych, and M. M. Telo da Gama, Eur. Phys. J. E **7**, 117 (2002).
 [14] M. Tasinkevych, N. M. Silvestre, P. Patrício, and M.M. Telo da Gama, Eur. Phys. J. E **9**, 341 (2002).
 [15] J. Fukuda and H. Yokoyama, Eur. Phys. J. E **4**, 389 (2001).
 [16] J. L. West, A. Glushchenko, G. Liao, Y. Reznikov, D. Andrienko, and M. P. Allen Phys. Rev. E **66**, 012702 (2002).
 [17] D. Andrienko, M. Tasinkevych, P. Patrício, and M. M. Telo da Gama submitted to Phys. Rev. E
 [18] S. Herminghaus *et al*, Adv. Mater. **11**, 1393 (1999); F. R. Service, Science **282**, 399 (1998).
 [19] P. G. de Gennes and J. Prost, *The Physics of Liquid Crystals* (Clarendon Press, Oxford, 1993), 2nd ed.
 [20] H. Imura and K Okano, Phys. Lett. A **42**, 2461 (1973).
 [21] A. Boulbitch, Europhys. Lett. **59**, 910 (2002).
 [22] M. Deserno and T. Bickel, Europhys. Lett. **62**, 767 (2003).
 [23] D. Andrienko, M. Tasinkevych, P. Patrício, M. P. Allen, and M. M. Telo da Gama Phys. Rev. E, Vol. 68, 051702 (2003).